Chemical Engineering Journal 169 (2011) 239–246

Contents lists available at ScienceDirect

Chemical Engineering Journal

journal homepage: www.elsevier.com/locate/cej

Porous ceramic mesoreactors: A new approach for gas–liquid contacting in multiphase microreaction technology

H.C. Aran[a], J.K. Chinthaginjala[b], R. Groote[c], T. Roelofs[c], L. Lefferts[b], M. Wessling[c], R.G.H. Lammertink[a,*]

[a] Soft Matter, Fluidics and Interfaces, Faculty of Science and Technology, University of Twente, P.O. Box 217, 7500AE Enschede, The Netherlands
[b] Catalytic Processes and Materials, Faculty of Science and Technology, University of Twente, P.O. Box 217, 7500AE Enschede, The Netherlands
[c] Membrane Science and Technology, Faculty of Science and Technology, University of Twente, P.O. Box 217, 7500AE Enschede, The Netherlands

ARTICLE INFO

Article history:
Received 27 July 2010
Received in revised form 15 October 2010
Accepted 1 November 2010

Keywords:
Microreactor
Gas–liquid–solid reactions
Membrane reactor
Surface modification
Ceramics

ABSTRACT

In this study a concept for gas–liquid–solid (G–L–S) microreaction technology was developed and optimized which ensures that the gaseous and liquid reactants directly meet at the solid catalyst surface with a simple contacting approach. Fabrication, catalyst deposition and surface modification steps were carried out to develop porous ceramic (alumina—Al_2O_3) mesoreactors. In order to realize liquid flow inside the intrinsically hydrophilic porous reactor channel and to obtain a stabilized gas–liquid–solid interface different surface modification (hydrophobization) strategies were successfully implemented. Catalytically active reactors with varying surface properties along the cross-section were obtained and their performance was tested for nitrite hydrogenation as a G–L–S model reaction. Results showed that the performance of the reactor could be drastically enhanced by tuning the surface properties. With the proposed concept, even at dilute concentrations of the gaseous reactant, the reactor performance remained constant.

1. Introduction

The development of miniaturized devices (in micro- and mesoscale) for carrying out chemical analysis and chemical reactions has shown a rapid improvement in the past years. A micro- or mesoreactor is a chemical reactor with a reduced dimensional scale (hydraulic diameter) which results in a very large surface/volume ratio. This large ratio provides enhanced heat and mass transfer enabling the development of more efficient processes (process intensification). Micro- and mesofluidic devices allow new chemical processes that were previously not applied in conventional systems. In addition they are sustainable by creating less waste, occupying less space, and enabling safer operation due to their small volume [1–5].

Multiphase reactions for gas–liquid (G–L) and heterogeneously catalyzed gas–liquid–solid (G–L–S) systems are conventionally performed in various types of reactors. The most widespread types include agitated tanks, slurry reactors, bubble or spray columns, and trickle-bed reactors [6]. Also membrane reactors have been intensively investigated due to their various advantages including well-defined contact regions and simple reactor design. In these types of reactors, the G–L interface is generally stabilized by the use of a pressure difference across the membrane (trans-membrane pressure) [7–14].

With the rapid developments in microreaction technology, some analogues of the macro-scale reactors became available for G–L and G–L–S reaction systems in the microscale [3,4,6,15,16]. Multiphase microreactors for these systems were classified by Hessel et al. [6] in two main types: *continuous* and *dispersed phase* microreactors. In the continuous phase reactors, both phases are separately fed to and withdrawn from the reactor without being dispersed into each other (e.g. the falling film microreactor). In the dispersed phase reactors, one phase is dispersed into the other one. Various flow patterns (e.g. Taylor flow and annular flow) are obtained in these microchannels. In these microreactors the G/L flow ratios have to be well controlled to create a stable interface between both phases [16]. For both continuous and dispersed phase systems, the gaseous reactant has to diffuse through a liquid film to reach the solid catalyst that can be immobilized on the microchannel wall.

The aim of the present work is to introduce a membrane reactor concept for G–L–S microreaction technology. The contact between gas and liquid for reaction purposes is achieved using membrane technology and selective wetting of porous ceramic membranes (Fig. 1).

The contacting between both phases takes place directly at the inner membrane surface, where the catalyst is immobilized. Using this continuous process concept, the gas phase composition can be kept constant along the full length of the reactor. Furthermore, no separation of gas and liquid reactants is necessary at the reactor outlet. The G–L interface and the positioning of the reaction area are controlled using surface modification (hydropho-

* Corresponding author. Tel.: +31 0534894798; fax: +31 0534894611.
E-mail address: r.g.h.lammertink@utwente.nl (R.G.H. Lammertink).

1385-8947/$ – see front matter © 2010 Elsevier B.V. All rights reserved.
doi:10.1016/j.cej.2010.11.005

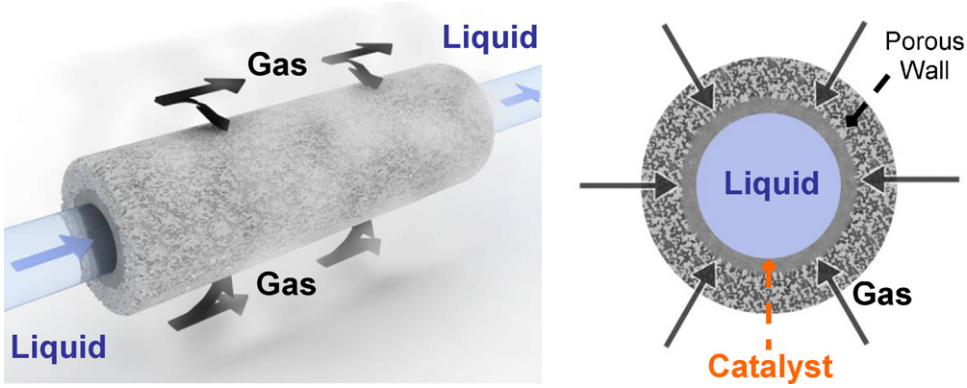

Fig. 1. Contacting concept of the porous ceramic mesoreactor for G–L–S reaction systems.

bization) techniques, as opposed to controlling trans-membrane pressure.

The heterogeneously palladium (Pd) catalyzed hydrogenation of nitrite ions in aqueous phase was chosen as G–L–S model reaction system for this study. The removal of nitrite (NO_2^-) and nitrate (NO_3^-) ions from groundwater is a relevant reaction from an environmental point of view. It can be carried out via biologic and catalytic hydrogenation processes. Due to the low reaction rates of the biologic processes, the catalytic hydrogenation process is mentioned to be more promising for the nitrite removal. Via the catalytic route the nitrite ions are converted to nitrogen (N_2) or the undesired product ammonia (NH_4^+) [17–21].

2. Experimental

2.1. Materials

Commercial α-Al_2O_3 hollow fibers InoCep M800 (Hyflux CEPAration Technologies (Europe)) with average pore diameter of 800 nm were used as membrane support in this study. The membrane fibers had an inner diameter of 2.8 mm, an outer diameter of 3.8 mm and they were prepared with a length of 13.5 cm. γ-Al_2O_3 (Alfa Aesar, 3 μm APS Powder), MilliQ-water, polyvinyl alcohol (PVA; Sigma–Aldrich, 99+% hydrolyzed) and acetic acid (Merck, pro analysi) were used for catalyst support preparation. Palladium(II) 2,4-pentanedione ($Pd(acac)_2$; Alfa Aesar, 34.7%) in toluene (Merck, ACS) was used as catalyst precursor solution. For the surface modification steps a perfluorinated octyltrichlorosilane (FOTS; Aldrich, 97%) and n-hexane as solvent (Merck, ACS) were used as received. An aqueous solution of Phenol Red sodium salt (Merck, ACS) was used as wetting indicator solution. Sodium nitrite ($NaNO_2$, Merck, ACS) was used as source for nitrite ions (NO_2^-).

2.2. Reactor preparation

The preparation of the porous ceramic mesoreactor consists of 3 main stages which are summarized in Fig. 2.

The inner surface of the commercial α-Al_2O_3 membrane (BET surface area: ~0.1 m^2/g) was coated with a γ-Al_2O_3 layer as catalyst support to increase the active surface area. For the coating procedure a standard recipe for the aqueous 20 wt% γ-Al_2O_3 suspension was used [22]. With the help of a syringe pump the suspension was fed into the fibers; the excess suspension was removed by flowing air (1 ml/min) through the fiber for 2 min. The coated samples were then dried in the oven at 50 °C for 1 h and then calcined at 600 °C for 2 h.

For the catalyst (Pd) deposition the samples were immersed into a precursor solution prepared of 300 mg of $Pd(acac)_2$ in 50 ml toluene for 24 h. The samples were removed from the solution and dried at 50 °C in air overnight. Finally the samples were calcined for 1 h at 250 °C in oxygen (O_2), followed by a 1 h reduction treatment with hydrogen (H_2) at the same temperature. For a second group of

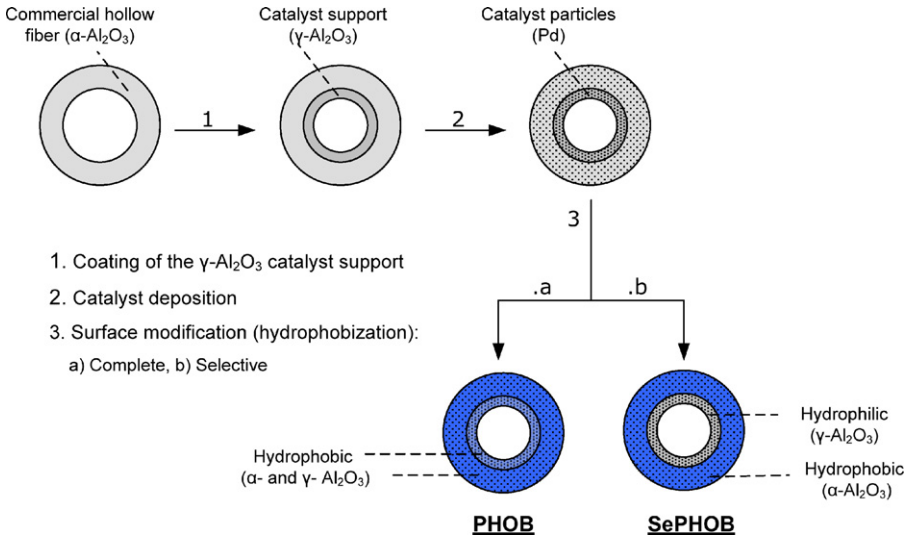

Fig. 2. Summary of the porous ceramic mesoreactor preparation steps: drawings represent the cross-sections of the membranes after each step.

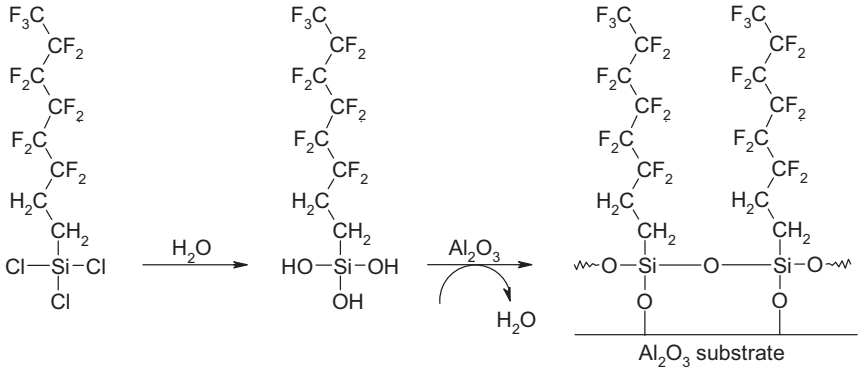

Fig. 3. Schematic representation for the surface modification of Al_2O_3 using FOTS, adapted from [23].

samples, the above mentioned treatments (immersion, drying, calcination and reduction) were repeated 3 times on the same sample to increase the palladium (Pd) content in the reactor walls.

Al_2O_3 hollow fiber membranes were hydrophobized by coating their surface with a fluorinated alkyl trichlorosilane (FOTS). The surface modification process of Al_2O_3 is illustrated in Fig. 3 [23].

Two different routes were performed for the surface modification: *complete* or *selective hydrophobization*.

Complete hydrophobization (liquid phase)

Adapted from Geerken et al. [24] the samples were immersed in a solution containing a few drops of FOTS in 40 ml n-hexane. They were kept in the solution for 1 h, taken out and placed in an oven at 100 °C for 1 h in order to realize the surface reaction between FOTS and Al_2O_3. After this reaction step the samples were rinsed with isopropanol to remove the excess FOTS on the membrane surface. The samples which were prepared using this method were labeled as "PHOB".

Selective hydrophobization (gas phase)

To prevent FOTS from reaching the γ-Al_2O_3 catalyst support on the inner part of the hollow fiber membrane, its ends were sealed (Fig. 4). The principle of FOTS gas phase deposition was adapted from previous work [25,26] and modified to the requirements in this study. The sealed membranes were placed in a desiccator and vacuum was applied to reach 6×10^{-2} mbar. After closing the vacuum pump FOTS was purged into the chamber for a short time (in the order of minutes). Then the FOTS compartment was closed and water vapor was introduced into the chamber for 10 s. The reaction of the FOTS with the surface took place at room temperature.

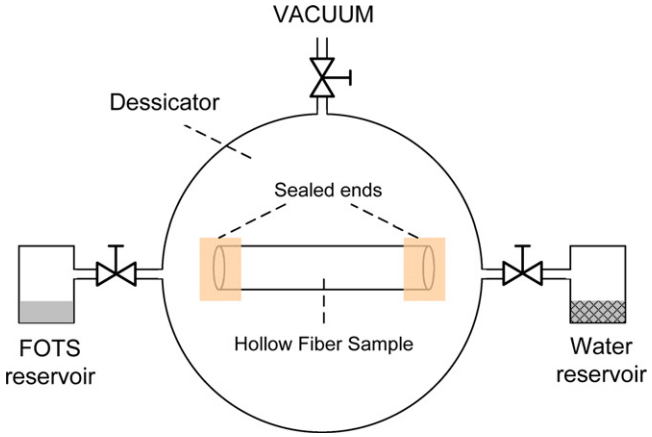

Fig. 4. Illustration of the selective hydrophobization setup and method.

These samples were labeled as "SePHOB" after this selective surface modification step.

2.3. Reactor characterization

The coating thickness and morphology were investigated using Scanning Electron Microscopy (SEM; JEOL TSM 5600). The samples were sputtered with a thin gold layer (Baltzers Union SCD 40) before imaging. To determine the active surface area of the γ-Al_2O_3 layer, BET surface area was measured using the N_2-adsorption isotherm obtained at 77 K (Micromeritics Tristar). The weight of the sample before and after the coating of the γ-Al_2O_3 layer was measured with an analytical balance.

The average Pd content on the samples with and without γ-Al_2O_3 catalyst supports was determined using X-ray fluorescence spectroscopy (XRF). The qualitative distribution of Pd at the cross-sections of the γ-Al_2O_3 layer was obtained by Scanning Electron Microscopy (LEO 1550 FEG-SEM) with energy dispersive X-ray analysis (EDX; Thermo Noran Vantage system). The dispersion and active particle size of Pd was determined by CO-chemisorption (Micromeritics, ChemiSorb 2750: Pulse Chemisorption system) at room temperature.

Contact angle measurements (OCA 15 Dataphysics) were carried out for each hydrophobization procedure. Due to the curved surface of the hollow fibers these measurements were performed on flat polished dense alumina wafers. Laplace pressures (for PHOB and SePHOB samples) at which the liquid (H_2O) wets the hydrophobic membrane from the tube to the shell side were measured. One end of the surface modified hollow fiber samples was sealed and water was pressurized from inside until water droplets appeared on the outer surface. This pressure difference at which the wetting occurred (Δp) can be correlated to the Laplace equation:

$$\Delta p = -\frac{2 \cdot \gamma_L \cdot \cos\theta}{r_{max}} \quad (1)$$

where γ_L is the surface tension of the liquid, θ is the contact angle of the liquid on the membrane material and r_{max} is the maximum pore radius of the membrane.

An aqueous Phenol Red sodium salt solution (~300 mg/l) was prepared and pumped through the surface modified reactors (PHOB and SePHOB) for a minimum time of 15 min, in order to visualize the wetting behavior throughout the sample. Then the samples were cut and the cross-sections were examined by optical microscopy (Zeiss Axiovert 40).

2.4. Reactor operation

The performance of the reactor was tested for heterogeneously catalyzed hydrogenation of nitrite (NO_2^-) ions over palladium cat-

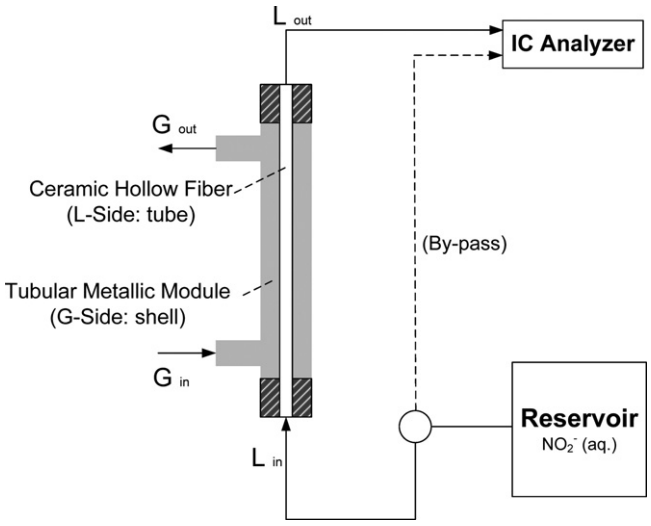

Fig. 5. Schematic representation of the experimental setup.

alyst in aqueous phase.

$$2NO_2^- + 3H_2 \xrightarrow{Pd} N_2 + 2OH^- + 2H_2O \quad (2)$$

$$2NO_2^- + 6H_2 \xrightarrow{Pd} 2NH_4^+ + 4OH^- \quad (3)$$

The conversion and the reaction rate of the nitrite ions were the main performance criteria. The production of the undesired product ammonia (NH_4^+) was also measured and used to calculate selectivity of the reaction. Selectivity to nitrogen (N_2) follows directly based on the well known fact that no other products are formed. The porous ceramic mesoreactors were placed into a stainless steel module with separate in- and outlets for liquid and gas (Fig. 5). The module was placed in a vertical position (liquid inlet at the bottom) inside an oven at 298 K. The liquid reactant (aqueous solution of NO_2^-) was pumped into the tube and the gaseous reactant (hydrogen: H_2, atmospheric pressure) was delivered to the shell side of the porous reactor.

Solutions of sodium nitrite with two different initial NO_2^- concentrations of ~11 and ~110 mg/l were prepared. The liquid reactants flow rates were chosen as 0.1 and 0.3 ml/min. The back pressure of the liquid before the entrance of the reactor was measured. The liquid outlet was connected to an ion chromatograph (IC; Dionex ICS 1000) and the NO_2^- and NH_4^+ concentrations were measured. The volumetric concentration of H_2 in the gas phase was varied between 1 and 100% using a mixture of H_2 and Argon (Ar) at different concentrations. The gas flow rate at the shell side was kept constant as 100 ml/min. The experimental parameters are summarized in Table 1.

Table 1
Experimental parameters: reactor types and operation conditions.

Reactor types	PHOB–SePHOB
Catalyst (Pd) deposition on reactor (times)	1–3
Reaction temperature (K)	298
Reactor volume (ml)	0.83
Initial nitrite concentrations (mg/l)	11–110
Liquid flow rates (ml/min)	0.1–0.3
Liquid flow back pressures (bar)	0.3–0.6
Gas flow rate (ml/min)	100
Volumetric H_2 concentrations in gas phase (%)	1–100

In addition to the above mentioned 3-Phase (G–L–S: H_2(g)–NO_2^-(aq)–Pd(s)) experiments, a 2-Phase (L–S: H_2(aq) and NO_2^-(aq)–Pd(s)) operation mode was tested where the liquid was presaturated with H_2 (in a mixture with Ar) in a reservoir and fed to the reactor. During the 2-Phase operation mode pure Ar gas was flown at the shell side of the reactor.

3. Results and discussion

3.1. Reactor characterization

The structures of the γ-Al_2O_3 coated ceramic hollow fiber used in this study are displayed in the SEM images in Fig. 6. The micrographs show that there is a clear difference in the morphology between the α- and γ-Al_2O_3 layers. The BET active surface area of the γ-Al_2O_3 support was found to be around 73 m^2/g, which is significantly higher compared to the commercial α-Al_2O_3 support (~0.1 m^2/g). The weight increase of the sample due to the coated support was measured to be 5.6 wt%. Thickness of the support was on average 80 μm.

Catalyst deposition was performed on samples with- and without γ-Al_2O_3 support coating. The overall weight percentage of Pd (measured by XRF) for the sample consisting of only α-Al_2O_3 was found to be 0.026 wt% and for the sample with additional γ-Al_2O_3 coating this value has increased to 0.073 wt%. This indicates that the amount of deposited catalyst could be significantly increased with the γ-Al_2O_3 coating due to the high surface area of this layer. For the samples with 3 times catalyst deposition the corresponding values increased to 0.12 and 0.26 wt%. It was observed that the Pd is mainly located in the γ-Al_2O_3 layer. The EDX results qualitatively showed a homogeneous distribution of Pd along the cross-section of the γ-Al_2O_3 coating. Both samples (containing additional γ-

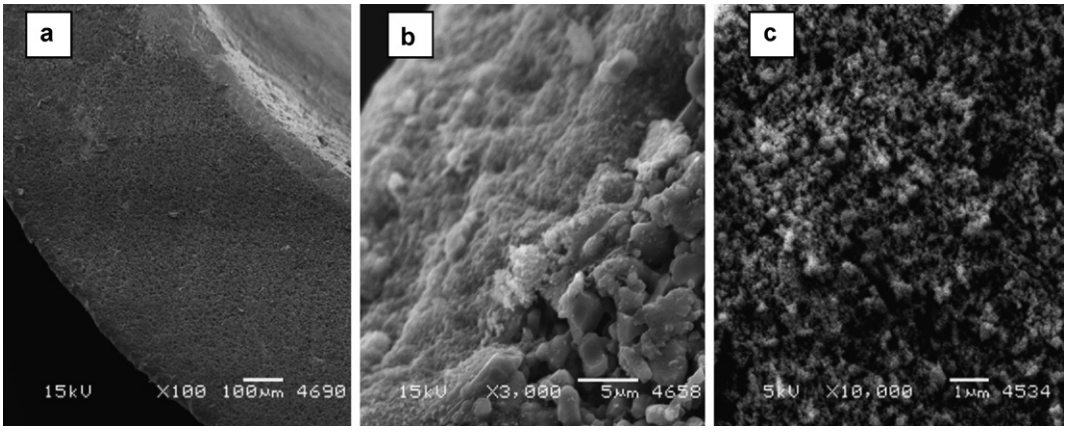

Fig. 6. SEM images of the ceramic membrane cross-section after γ-Al_2O_3 catalyst support coating: (a and b) α-Al_2O_3/γ-Al_2O_3 intersection and (c) porous structure of the γ-Al_2O_3 layer.

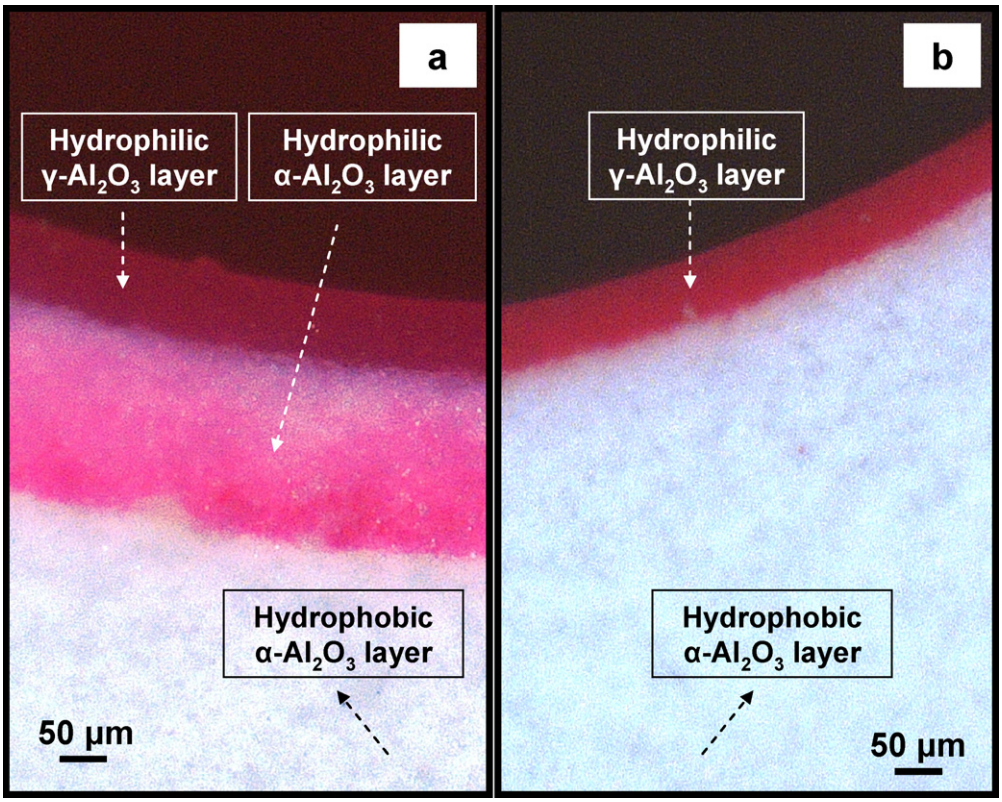

Fig. 7. Visualization of the wetting behavior for the selectively hydrophobized (SePHOB) hollow fibers. Optical microscope cross-section images for tracking the liquid flow, indicating where the liquid reaches. (a) Partially wetted α-Al_2O_3 layer and (b) completely hydrophobic α-Al_2O_3 and hydrophilic γ-Al_2O_3 layers.

Al_2O_3 coating) with 1 and 3 times catalyst deposition were used in this work as reactors in order to study the effect of catalyst loading on the reactor performance. These samples were referred as Pd loading = 0.073 wt% (1 time deposition) and Pd loading = 0.26 wt% (3 time deposition) in Section 3.2.

The Pd dispersion of a sample (measured by CO-chemisorption) with α- and γ-Al_2O_3 layer was 7.9% (average particle size = 14 nm) after a single exposure for Pd deposition, and 6.5% (average particle size = 17 nm) after 3 times repetitive Pd deposition. However, it must be noted that these XRF and CO-chemisorption results were obtained for the entire sample (α- and γ-Al_2O_3) and not specifically for the γ-Al_2O_3 layer which is relevant for catalytic activity.

Contact angles were measured on dense flat Al_2O_3 samples after the hydrophobization step (for both liquid and gas phase hydrophobization methods). For both samples, the contact angles were around 115° which confirms that both methods were successful in hydrophobizing Al_2O_3.

The wetting behavior of the porous ceramic fibers modified by the complete (PHOB) and selective (SePHOB) hydrophobization methods were investigated using an aqueous Phenol Red solution as wetting indicator. Samples without any surface modification were completely wetted by the indicator solution within a few seconds. For the PHOB (completely hydrophobized) sample no considerable coloring in the cross-sections along the length of the fiber was observed indicating that the entire sample was hydrophobized. For the SePHOB (selectively hydrophobized) samples wetting was observed only in the γ-Al_2O_3 layer. This method apparently allows hydrophobizing only the α-Al_2O_3 selectively while γ-Al_2O_3 layer remains hydrophilic. Apparently, by sealing the ends of the fiber the direct transport of FOTS to the inner membrane surface and therefore hydrophobization of the γ-Al_2O_3 layer could be prevented.

To determine the parameters for the selective hydrophobization (SePHOB) procedure, the FOTS exposure time was varied and different degrees of wetting were observed (Fig. 7). In samples with shorter exposure times wetting was seen also in the α-Al_2O_3 layer (Fig. 7a) which indicates that some regions also in this layer remained hydrophilic. But for longer FOTS exposure times it was observed that the α-Al_2O_3 layer became completely hydrophobic (Fig. 7b). Also the wetting behavior was identical along the length of the fiber. Further increase of the exposure time on the order of minutes resulted in the same wetting behavior as in Fig. 7b; the γ-Al_2O_3 layer remained still hydrophilic. These results indicate that gas phase modification of the γ-Al_2O_3 layer is a slower process compared to modifying the α-Al_2O_3 layer. Most likely, this results from the adsorption of FOTS at the α-Al_2O_3 layer, combined with the smaller pore sizes and high surface area of the γ-Al_2O_3 layer (Fig. 6). Probably, the diffusion of FOTS is slower due to the smaller pores and larger amount of FOTS is needed to cover the high surface area in this layer.

Laplace pressures of the PHOB and SePHOB samples were measured. These pressures were 1.7 bar for the PHOB samples and 1.1 bar for the SePHOB samples. For the PHOB sample the liquid has to wet the hydrophobic γ-Al_2O_3 layer first, whereas for the SePHOB sample the hydrophilic γ-Al_2O_3 layer is already wetted, explaining the higher Laplace pressure for the PHOB sample. The measured Laplace pressure for the SePHOB sample is comparable to the value predicted from the Laplace equation for the α-Al_2O_3 layer, ~1.5 bar for a maximum pore radius of 800 nm. However, a higher wetting pressure than 1.7 bar should be expected for the PHOB sample due to the significantly smaller pore sizes in the γ-Al_2O_3 layer (Fig. 6). This low value indicates the presence of defects in the γ-Al_2O_3 layer, such as macrovoids (large pores), cracks or incomplete hydrophobization.

It must be noted that both of the measured Laplace pressures are higher than the back pressures (Table 1) for each flow rate, which ensures a stable gas–liquid interface without the liquid reactant leaking to the gas side.

Table 2
Effect of the surface properties on the reactor performance: NO_2^- conversions and reaction rates for PHOB and SePHOB reactors (initial nitrite concentration = ~11 mg/l, H_2 concentration = 100%, Pd loading = 0.073 wt%).

L-Flow rate (ml/min)	Reactor	NO_2^- conversion	Reaction rate ($\times 10^5$ mmol/min)
0.1	PHOB	25%	0.6
	SePHOB	71%	1.8
0.3	PHOB	11%	0.8
	SePHOB	39%	2.8

3.2. Reactor performance

The catalytic performance of the obtained reactors was investigated using heterogeneously Pd catalyzed hydrogenation of nitrite in aqueous phase as a model reaction. The main performance criteria were the nitrite conversion and the reaction rates which were determined by measuring the initial and final concentrations of the nitrite ions before and after the reactor.

In order to determine the influence of the surface properties on the reactor performance two reactors (Pd loading = 0.073 wt%) with different surface properties were tested:

- PHOB (hydrophobic α- and γ-Al_2O_3 layers),
- SePHOB (hydrophobic α-Al_2O_3 and hydrophilic γ-Al_2O_3 layers).

Table 2 shows the overall conversions of nitrite ions and reaction rates as a function of the liquid flow rate for both reactors. It can be seen that the performance increased drastically using the SePHOB reactor. These results clearly show the improvement achieved by altering wall wetting conditions. This significant increase in the nitrite conversions can be explained by the increased contact interface between the liquid reactant and the Pd catalyst. While in the PHOB reactor the liquid reactant was in contact with a hydrophobic γ-Al_2O_3 catalyst support preventing efficient contact between the nitrite solution and the active Pd, in the SePHOB reactor the liquid reactant was able to contact the complete hydrophilic γ-Al_2O_3 layer resulting in significantly higher conversion values. The measured selectivity values to ammonia were found to be approximately 53% for the PHOB and 40% for the SePHOB reactor.

The effect of the H_2 concentration in the gas phase of the reactor was investigated for the PHOB and SePHOB reactors (Pd loading = 0.073 wt%). The flow rate of the gas phase was kept constant, but the volumetric concentration of gaseous reactant H_2 in the gas flow was varied between 1% and 100% (H_2 partial pressures) using Ar as diluting agent.

As can be seen in Fig. 8, the performance of the reactor remained constant with decreasing hydrogen concentration. A slight decrease in conversions was observed when the H_2 concentration dropped below 5%. The selectivity to the undesired product NH_4^+ decreased very slightly with decreasing H_2 concentration. Results show that even at low values of H_2 concentration, the gaseous reactant could easily reach the reaction area (γ-Al_2O_3 layer) through the non-wetted pores of the hydrophobic α-Al_2O_3. This concept ensures negligible mass transport limitations for the gas reactant. Even at low hydrogen concentrations in the gas phase, enough hydrogen is provided to maintain the reaction with dissolved nitrite (~0.24 mmol/l).

The initial nitrite concentration in the liquid phase was increased from 11 to 110 mg/l. The experiments were carried out with the SePHOB reactor for different H_2 concentrations (5–100%) and at two different liquid flow rates (0.1 and 0.3 ml/min).

For increased nitrite concentrations, even though the nitrite conversion values have decreased compared to the experiments with lower nitrite concentration (Table 3), the reaction rates have significantly increased. The selectivity of the reaction towards ammonia was approximately 24%. In addition, with the variation of the H_2 concentration (down to 5%) it was observed that the nitrite conversion performances again remained constant over the full concentration range. These high nitrite reaction rates at high initial nitrite concentration (~2.40 mmol/l) show that the continuous supply of the gas phase provides enough H_2 to the reaction area even though H_2 has a low solubility in water (~0.78 mmol/l at 25 °C [27]). The apparent order in H_2 for this configuration is zero, suggesting that the Pd surface is almost completely covered with H-atoms. Apparently, this way of introducing H_2 is extremely efficient. The turn-over-frequency (TOF), representing the amount of NO_2^- ions converted per surface-Pd-atom, was calculated for the SePHOB reactor (Pd loading = 0.073 wt%, initial NO_2^- concentration = ~11 mg/l) to be $\sim 0.5 \times 10^{-3}$ s^{-1}. This value is relatively small compared to the TOF obtained in previous work ($\sim 3.4 \times 10^{-3}$ s^{-1}) for γ-Al_2O_3 supported Pd catalyst [20]. However, this is not a surprise when considering the high level of conversion as reported in Table 3, as compared to differential experiments [20]. Therefore, the TOF obtained here is an averaged value due to variations in both nitrite concentration as well as pH along the axis of the reactor.

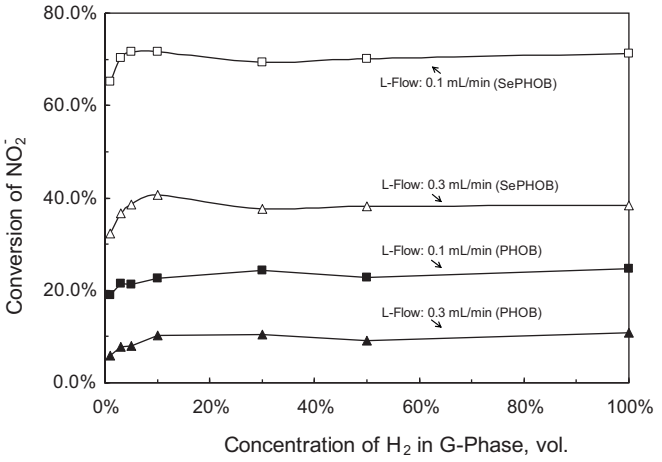

Fig. 8. The effect of the hydrogen concentration on the reactor performance. Nitrite conversion values for PHOB and SePHOB reactors (initial nitrite concentration = ~11 mg/l, Pd loading = 0.073 wt%).

In order to investigate the effect of the amount of catalytically active sites on the membrane wall, two reactors with two different catalyst loadings were tested. SePHOB reactors with 0.073 wt% Pd loading and with 0.260 wt% Pd loading were used and the tests were carried out for initial nitrite concentrations of ~11 and ~110 mg/l.

Fig. 9 illustrates the obtained nitrite conversions for each reactor under the different process conditions. Higher conversion values were obtained for the reactor with higher catalyst loading. The increments in conversions and reaction rates for each flow rate were more evident for higher initial nitrite concentrations (from 9.9 and 13.7×10^{-5} mmol/min to 15.0 and 22.7×10^{-5} mmol/min) because of the lower conversion levels (closer to differential conditions), where the concentration gradients along the reactor length are less significant. These results show that the performance can be

Table 3
Effect of initial nitrite concentration on the performance of the SePHOB reactor: NO_2^- conversions and reaction rates (initial nitrite concentrations = ~11 mg/l and ~110 mg/l, H_2 concentration = 100%, Pd loading = 0.073 wt%).

Initial NO_2^- concentration	L-flow rate (ml/min)	NO_2^- conversion	Reaction rate ($\times 10^5$ mmol/min)
~11 mg/l	0.1	71%	1.8
	0.3	39%	2.8
~110 mg/l	0.1	40%	9.9
	0.3	18%	13.7

Table 4
Comparison of 2-Phase and 3-Phase Systems for a SePHOB reactor (initial nitrite concentration = ~11 mg/l, Pd loading 0.260 wt%).

Operation mode	L-flow rate (ml/min)	Nitrite conversion (%)		H_2 conversion (%)		Selectivity to NH_4^+ (%)	
		$x(H_2)$ (vol.)		$x(H_2)$ (vol.)		$x(H_2)$ (vol.)	
		10%	100%	10%	100%	10%	100%
2-Phase	0.1	11	72	51	47	4	36
	0.3	14	53	72	40	5	60
3-Phase	0.1	80	80	–	–	37	40
	0.3	46	46	–	–	42	38

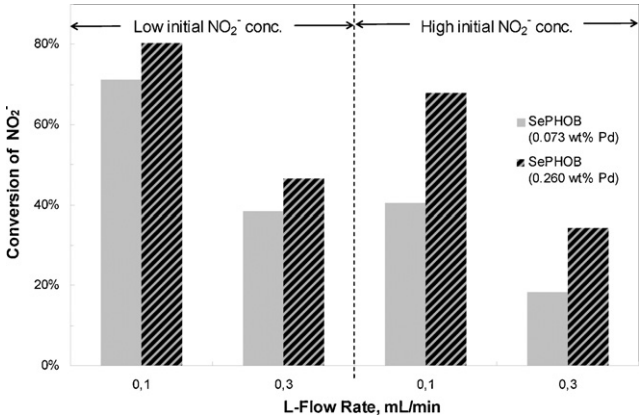

Fig. 9. Effect of catalyst loading on the reactor performance. Nitrite conversion values for SePHOB reactors with 0.073 wt% and 0.260 wt% Pd loading (initial nitrite concentration = ~11 (low) and ~110 (high) mg/l, H_2 concentration = 100%).

improved by increasing the amount of Pd catalyst in the selectively hydrophobized reactor. However, the extent of the increase is far smaller than the increase in Pd loading, which is due to the high conversion levels and hence a significantly lower concentration in the downstream of the reactor (integral conditions), as well as to the decreased dispersion of Pd.

The nitrite conversions of the proposed 3-Phase concept were compared with the performance of a 2-Phase system for the same reaction using the same reactor. In the 2-Phase system the initial nitrite feed solution was saturated with the gaseous reactant of H_2 or its mixtures with Ar. For this mode, both reactants (NO_2^- and H_2) are dissolved in water (L) reacting on the catalyst (S) surface and no reactant (H_2) is fed from the gas phase. The solution was fed into the same porous ceramic mesoreactor. For this comparison, two different liquid flow rates (0.1 and 0.3 ml/min) and two different H_2 concentrations ($x(H_2)$) were used. Tests were carried out in the SePHOB reactor with 0.260 wt% Pd loading. The conversion values of the presaturated H_2 in the liquid phase were calculated for the 2-Phase experiments from the reaction stoichiometry ((2) and (3)) considering the selectivity of the reaction.

The experiments clearly show (Table 4) that the performance of the 2-Phase system is more sensitive to the H_2 concentration. For 10% H_2 concentration, the conversion values dropped drastically in the 2-Phase system while for 100% H_2 concentration these values were in the same range for both operation modes. The decrease of the conversions for low H_2 concentrations at 2-Phase operation mode is caused by depletion (exhaustion) of dissolved hydrogen in the liquid phase along the reactor axis. Presaturation with 10% H_2 (partial pressure = 0.1 bar) results in ~0.078 mmol/l dissolved H_2 at 25 °C, which is not sufficient to convert the dissolved nitrite (~0.24 mmol/l) completely. These results demonstrate the key advantage of the proposed 3-Phase contacting system, where a continuous supply of the gaseous reactant along the full length of the reactor via the membrane prevents depletion of the gaseous reactant, without dispersing the gas in the liquid phase.

4. Conclusions and future work

In this study, a contacting concept for gas–liquid–solid (G–L–S) microreaction technology was studied. Porous ceramic mesoreactors in tubular geometry with controllable wetting properties and catalytic activity were developed. The reactors were characterized and the proposed reactor concept was applied for catalytic hydrogenation of nitrite. The developed reactors showed promising performance for this environmentally relevant catalytic reaction system.

Main conclusions of this study are as follows:

- The wetting behavior for the liquid reactant on the catalyst surface and the position of the G–L interface can easily be tuned and a stable G–L–S interface for heterogeneously catalyzed reaction processes can be obtained applying surface modification (hydrophobization) techniques.
- Reactors prepared with selective hydrophobization techniques (SePHOB), in which the membrane support is hydrophobized while the catalyst support remains hydrophilic, proved to be the most effective configuration for this reactor approach.
- The performance of the reactor remained constant even when the gaseous reactant (H_2) concentration was decreased. This concept provides very efficient transfer of H_2 by continuous addition through the membrane, allowing operating at low partial pressures of H_2.

Membrane technology shows to have a promising potential to be implemented for microreactors in G–L–S reaction systems. Despite the above mentioned conclusions some issues remain to be investigated. Ongoing work is focused on different configurations inside the reactor such as the influence of different thicknesses of the catalyst support layer, effect of the decreased internal diameters (microscale) and mixing strategies to increase the performance.

Acknowledgements

This work was financially supported by Stichting voor de Technische Wetenschappen (STW, Project 07569). We are grateful to B. Geerdink, K. Altena -Schildkamp and J.A.M. Vrielink for analysis and technical support. The authors also greatly acknowledge D. Salamon and J.M. Jani for the fruitful discussions and J. Bennink (Tingle.nl) for making the illustrations.

References

[1] A. Gavriilidis, P. Angeli, E. Cao, K.K. Yeong, Y.S.S. Wan, Technology and applications of microengineered reactors, Chem. Eng. Res. Des. 80 (2002) 3–30.
[2] K.F. Jensen, Microreaction engineering—is small better? Chem. Eng. Sci. 56 (2001) 293–303.
[3] M.N. Kashid, L. Kiwi-Minsker, Microstructured reactors for multiphase reactions: state of the art, Ind. Eng. Chem. Res. 48 (2009) 6465–6485.
[4] G.N. Doku, W. Verboom, D.N. Reinhoudt, A. van den Berg, On-microchip multiphase chemistry—a review of microreactor design principles and reagent contacting modes, Tetrahedron 61 (2005) 2733–2742.
[5] P.L. Mills, D.J. Quiram, J.F. Ryley, Microreactor technology and process miniaturization for catalytic reactions—a perspective on recent developments and emerging technologies, Chem. Eng. Sci. 62 (2007) 6992–7010.

[6] V. Hessel, P. Angeli, A. Gavriilidis, H. Lowe, Gas–liquid and gas–liquid–solid microstructured reactors: contacting principles and applications, Ind. Eng. Chem. Res. 44 (2005) 9750–9769.
[7] J. Coronas, J. Santamaría, Catalytic reactors based on porous ceramic membranes, Catal. Today 51 (1999) 377–389.
[8] K. Dittmeyer, M. Svajda, Reif, A review of catalytic membrane layers for gas/liquid reactions, Top. Catal. 29 (2004) 3–27.
[9] A.G. Dixon, Recent research in catalytic inorganic membrane reactors, Int. J. Chem. React. Eng. 1 (2003) 1–35.
[10] A. Julbe, D. Farrusseng, C. Guizard, Porous ceramic membranes for catalytic reactors—overview and new ideas, J. Membr. Sci. 181 (2001) 3–20.
[11] J. Peureux, M. Torres, H. Mozzanega, A. Giroir-Fendler, J.A. Dalmon, Nitrobenzene liquid-phase hydrogenation in a membrane reactor, Catal. Today 25 (1995) 409–415.
[12] M. Vospernik, A. Pintar, G. Bercic, J. Batista, J. Levec, Potentials of ceramic membranes as catalytic three-phase reactors, Chem. Eng. Res. Des. 82 (2004) 659–666.
[13] M. Vospernik, A. Pintar, G. Bercic, J. Levec, Experimental verification of ceramic membrane potentials for supporting three-phase catalytic reactions, J. Membr. Sci. 223 (2003) 157–169.
[14] R. Dittmeyer, V. Höllein, K. Daub, Membrane reactors for hydrogenation and dehydrogenation processes based on supported palladium, J. Mol. Catal. A: Chem. 173 (2001) 135–184.
[15] G. Chen, J. Yue, Q. Yuan, Gas–liquid microreaction technology: recent developments and future challenges, Chin. J. Chem. Eng. 16 (2008) 663–669.
[16] V. Hessel, S. Hardt, H. Loewe, Chemical Micro Process Engineering, Wiley–VCH, Weinheim, 2003.
[17] A. Pintar, G. Bercic, J. Levec, Catalytic liquid-phase nitrite reduction: kinetics and catalyst deactivation, AIChE J. 44 (1998) 2280–2292.
[18] K.D. Vorlop, T. Tacke, Erste Schritte auf dem Weg zur edelmetallkatalysierten Nitrat- und Nitrit-Entfernung aus Trinkwasser, Chem. Ing. Tech. 61 (1989) 836–837.
[19] S.D. Ebbesen, B.L. Mojet, L. Lefferts, In situ ATR-IR study of nitrite hydrogenation over Pd/Al_2O_3, J. Catal. 256 (2008) 15–23.
[20] J.K. Chinthaginjala, L. Lefferts, Support effect on selectivity of nitrite reduction in water, App. Cat. B: Env. 101 (2010) 144–149.
[21] J.K. Chinthaginjala, J.H. Bitter, L. Lefferts, Thin layer of carbon-nano-fibers (CNFs) as catalyst support for fast mass transfer in hydrogenation of nitrite, Appl. Catal. A: Gen. 383 (2010) 24–32.
[22] R. Zapf, C. Becker-Willinger, K. Berresheim, H. Bolz, H. Gnaser, V. Hessel, G. Kolb, P. Löb, A.K. Pannwitt, A. Ziogas, Detailed characterization of various porous alumina-based catalyst coatings within microchannels and their testing for methanol steam reforming, Chem. Eng. Res. Des. 81 (2003) 721–729.
[23] M.J. Geerken, T.S.v. Zanten, R.G.H. Lammertink, Z. Borneman, W. Nijdam, v.C.J.M. Rijn, M. Wessling, Chemical and thermal stability of alkylsilane based coatings for membrane emulsification, Adv. Eng. Mater. 6 (2004) 749–754.
[24] M.J. Geerken, R.G.H. Lammertink, M. Wessling, Tailoring surface properties for controlling droplet formation at microsieve membranes, Colloids Surf. A 292 (2007) 224–235.
[25] H. Rathgen, Superhydrophobic surfaces: from fluid mechanics to optics, Doctoral Thesis, University of Twente, Enschede, 2008.
[26] T.M. Mayer, M.P. de Boer, N.D. Shinn, P.J. Clews, T.A. Michalske, Chemical vapor deposition of fluoroalkylsilane monolayer films for adhesion control in microelectromechanical systems, J. Vac. Sci. Technol. B18 (2000) 2433–2440.
[27] D.R. Lide, W.M. Haynes (Eds.), CRC Handbook of Chemistry and Physics, 90th ed., CRC Press/Taylor and Francis, Boca Raton, FL, 2010 (Internet Version).